PAPER

Finding non-classical critical nuclei and minimum energy path of Cu precipitates in Fe–Cu alloys

View the article online for updates and enhancements.

Related content

Finding non-classical critical nuclei and minimum energy path of Cu precipitates in Fe–Cu alloys

Boyan Li[1] ⬩, **Lei Zhang**[2,6], **Chengliang Li**[3], **Qiulin Li**[4], **Jun Chen**[3], **Guogang Shu**[3], **Yuqing Weng**[5], **Ben Xu**[1,6] **and Wei Liu**[1,6]

[1] School of Materials Science and Engineering, Tsinghua University, People's Republic of China
[2] Beijing International Center for Mathematical Research, Center for Quantitative Biology, Peking University, Beijing 100871, People's Republic of China
[3] China Nuclear Power Engineering Co., Ltd, Shenzhen, People's Republic of China
[4] Graduate School at Shenzhen, Tsinghua University, Shenzhen, People's Republic of China
[5] Central Iron & Steel Research Institute, Beijing, People's Republic of China

E-mail: zhangl@math.pku.edu.cn, xuben@mail.tsinghua.edu.cn and liuw@mail.tsinghua.edu.cn

CrossMark

Abstract

For most steels, the aging- or radiation-induced hardenability of Cu precipitates has been concerned for many years. Experiments show that Fe–Cu alloys undergo aging- or radiation- induced phase separation into Cu-rich precipitates, resulting in property degradation processes. In this work, we developed a model integrating constrained string method and phase-field approaches to investigate the non-classical critical nuclei and minimum energy path of Cu precipitates. The Fe–Cu binary alloy is taken as a model system. The free energies used in the phase-field model are from CALPHAD. The simulation results demonstrated that the formation of Cu stable clusters undergo an energy barrier and the predicted thermodynamic properties of the critical nucleus which are related to temperature and Cu overall concentration, in good agreement with the theoretical calculation as well as experimental observations.

Keywords: Fe–Cu alloys, non-classical clustering, minimum energy path, phase field model, constrained string method

(Some figures may appear in colour only in the online journal)

---

[6] Authors to whom any correspondence should be addressed.

1. Introduction

For most steels, the aging- or radiation-induced hardenability of Cu precipitates has been concerned for many years [1]. These Cu precipitates can not only strengthen the hardness of low-carbon steels [2], but also result in important materials property degradation processes, especially in reactor pressure vessel [3]. For instance, Fe–Cu alloys undergo aging- or radiation- induced phase separation into Cu-rich precipitates, and the addition of Mn and Ni in these steels can accelerate this progress [4]. Such phase separation leads to material property degradation including embrittlement and reduction of ductile to brittle transition temperatures [3]. On the other hand, Cu is a common element in steels with a low solubility in α phase at a lower temperature. It is easier for Cu-rich clusters to form at a lower temperature driven by thermodynamics. In the dynamic process, the diffusion coefficient of Cu decreases with the decrease of temperature. Extra defects induced by radiation such as vacancies, or high temperature can accelerate the clustering of Cu-rich precipitates [5–8]. Therefore, it is crucial to understand the thermodynamic properties of critical nuclei for predicting microstructure evolution and material property degradation.

Phase separation in Fe–Cu alloys takes place through two mechanisms: (1) Cu-rich phase nucleation and growth and (2) spinodal decomposition, which is determined by the temperature and Cu overall concentration. However, modeling and simulation of nucleation is believed to be one of the most challenging problems in materials. The phase field model is a powerful simulation tool that can account for the effect of short and long range interaction energies on phase stability and microstructure evolution as well anisotropic thermodynamic and kinetic properties [9–14]. However, it is a challenge for the phase field approach to simulate the nucleation process by solving Allen–Chan or Cahn–Hilliard equations because it assumes that the microstructure evolution is driven by the energy minimization while the nucleation needs to overcome a minimum thermodynamic energy barrier. Moreover, the critical nucleus is a saddle point configuration along the minimum energy path (MEP), and it is difficult to be captured from physical experiments because it only appears transiently at very fast time scales. Therefore, there have been many efforts to study the critical nucleus and nucleation events in order to simulate the phase separation [15–25].

In this work, we will quantitatively calculate the critical nucleus by coupling the phase field model with the constrained string method. A detailed description of the model will be presented in section 2, including the phase field model and the string method used for finding the non-classical critical nuclei and MEP of Cu precipitates. The thermodynamic and kinetic properties of Fe–Cu alloys are described as well. The simulation results of critical nucleus radius, concentration of Cu in a critical nucleus, energy barrier and the MEP of Cu-rich precipitates are presented and discussed in section 3.

2. Description of the model

2.1. Phase field model

In this model, the precipitation of Cu is described by Cu concentration, $C_{Cu}(\mathbf{r}, t)$, where $\mathbf{r} = (r_1, r_2, r_3)$ is the spatial coordinate and t is the evolution time. Considering the high solubility of Cu and the low thermal equilibrium vacancy concentration in Fe–Cu system, we can ignore the vacancy concentration in this model. As a result, the concentration of Fe is $1 - C_{Cu}$. The total energy of the system usually includes chemical free energies, interfacial energies and long-range interaction energies, such as elastic energy and static electric energy. For our Fe–Cu alloys, the total free energy can be written as:

$$E(C_{\mathrm{Cu}}, \ \varepsilon_{ij}^*, \ T) = \int_V \left[\frac{NA_0}{\Omega_0} G(C_{\mathrm{Cu}}, \ T) + \frac{\kappa_{\mathrm{Cu}}}{2} |\nabla C_{\mathrm{Cu}}|^2 + E_{\mathrm{elas}}(\varepsilon) \right] dV, \tag{1}$$

where $N = 6.022 \times 10^{23}$ (atom mol^{-1}), is the Avocado's constant; constant $A_0 = 1.602 \times 10^{-19}$ (J eV^{-1}); $\Omega_0 = 1.4087 \times 10^{-5}$ (m^3 mol^{-1}), is the molar volume of bcc Fe; $G(C_{\mathrm{Cu}}, \ T)$ is the chemical free energy density per atom in electron volts (eV); T is the temperature (K); κ_{Cu} is the interfacial energy coefficient; $E_{\mathrm{elas}}(\varepsilon)$ is the elastic energy term induced from the coherent phase separation in the α phase, $E_{\mathrm{elas}}(\varepsilon) = YV_m\varepsilon^2(C_{\mathrm{Cu}})$. Where $Y = 2.14 \times 10^{11}$ (Pa), is the energy function expressed using elastic constants, $V_m = 7.09 \times 10^{-6}$(m^3 mol^{-1}), is the molar volume. $\varepsilon(C_{\mathrm{Cu}}) = \mu_{\mathrm{Cu}}(C_{\mathrm{Cu}} - C_{\mathrm{Cu0}})$, is the eigen-strain. μ_{Cu} is the lattice mismatch. These parameters can be obtained from [26]. C_{Cu0} is the average Cu concentration. V is the volume of the considered system. $\nabla = \left(\frac{\partial}{\partial r_1}, \frac{\partial}{\partial r_2}, \frac{\partial}{\partial r_3} \right)$, is the gradient operator.

According to the Cahn–Hilliard non-classical nucleation theory, the temporal evolution of the concentration of Cu can be written as:

$$\frac{\partial C_{\mathrm{Cu}}}{\partial t} = -\nabla \cdot \left(-M\nabla \frac{\delta E(C_{\mathrm{Cu}}, \ \varepsilon_{ij}^*, \ T)}{\delta C_{\mathrm{Cu}}} \right) = \nabla \cdot M\nabla \left(\frac{NA_0}{\Omega_0} \cdot \frac{\partial G(C_{\mathrm{Cu}}, \ T)}{\partial C_{\mathrm{Cu}}} - \kappa_{\mathrm{Cu}}\nabla^2 C_{\mathrm{Cu}} \right), \tag{2}$$

where M is the mobility of Cu and it is related to Cu element diffusion coefficient:

$$M = \frac{D\Omega_0}{RT}, \tag{3}$$

where D is the diffusivity of Cu, and R is the gas constant of $R = 8.314$ J mol^{-1} K^{-1}.

In this phase field model, the following normalizations are used:

$$r^* = \frac{r}{l_0}, \ \nabla^* = \left(\frac{\partial}{\partial r_1^*}, \frac{\partial}{\partial r_2^*}, \frac{\partial}{\partial r_3^*} \right) = l_0\nabla,$$

$$t^* = \frac{t}{t_0}, \ \ t_0 = \frac{l_0^2\Omega_0}{NA_0M}, \ \kappa_{\mathrm{Cu}}^* = \frac{\Omega_0}{NA_0l_0^2}\kappa_{\mathrm{Cu}},$$

where l_0 is a characteristic length. Then the equation (2) can be written as:

$$\frac{\partial C_{\mathrm{Cu}}}{\partial t^*} = \nabla^{*2} \left(\frac{\partial G(C_{\mathrm{Cu}}, \ T)}{\partial C_{\mathrm{Cu}}} - \kappa_{\mathrm{Cu}}^*\nabla^{*2}C_{\mathrm{Cu}} \right). \tag{4}$$

2.2. Chemical free energy

To predict Cu cluster and solve the phase field equation (4), we need the chemical free energy density $G(C_{\mathrm{Cu}}, T)$. Due to the efforts made by many researchers, the analytical free energy density has now become available for the Fe–Cu system [27, 28]. The chemical free energy density (Gibbs free energy) of α (bcc) phase for Fe–Cu binary alloy with magnetic contribution is described as:

$$G(C_{\mathrm{Cu}}, T) = {}^0G + {}^EG + {}^{\mathrm{mg}}G + RT[C_{\mathrm{Cu}}\ln C_{\mathrm{Cu}} + (1 - C_{\mathrm{Cu}})\ln(1 - C_{\mathrm{Cu}})], \tag{5}$$

$${}^0G = {}^0G_{\mathrm{Cu}}C_{\mathrm{Cu}} + {}^0G_{\mathrm{Fe}}(1 - C_{\mathrm{Cu}}), \tag{6}$$

$${}^EG = L_{\mathrm{Cu,Fe}}C_{\mathrm{Cu}}(1 - C_{\mathrm{Cu}}), \tag{7}$$
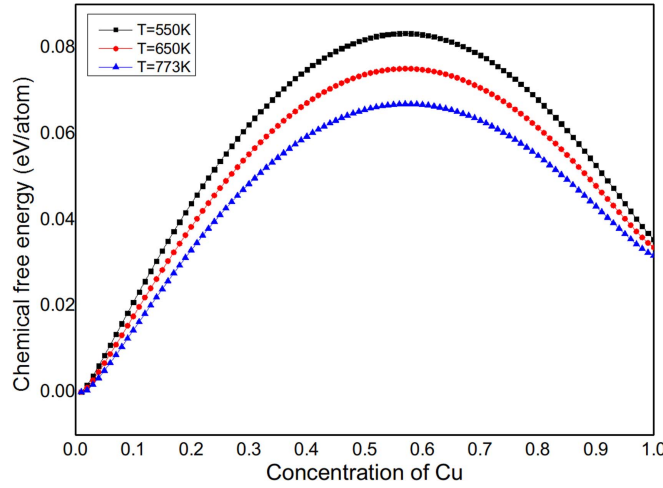
Figure 1. Chemical free energy density of Fe–Cu alloys at different temperatures.

$$^{\mathrm{mg}}G = RT \ \ln(\beta^\alpha + 1)f(\tau), \ \ \tau = \frac{T}{T_{\mathrm{C}}}, \tag{8}$$

where ^0G is the ideal mixing Gibbs free energy and ^0G_i is the Gibbs free energy of pure element i ($i = $ Cu, Fe) with bcc crystal structure in terms of temperature [29]. ^EG is the excess free energy caused by the heat of mixing, and $^{\mathrm{mg}}G$ is the magnetic contribution to the Gibbs free energy. R and T are gas constant of $R = 8.314$ J mol^{-1} K^{-1} and the absolute temperature (K), respectively. The interaction parameter $L_{\mathrm{Cu,Fe}}$, the Curie temperature T_{c}, and the atomic moment β^α are available from the thermodynamic database of equilibrium phase diagrams and have been assessed by Miettinen [30]:

$$^0G_{\mathrm{Fe}} = 0, \ \ ^0G_{\mathrm{Cu}} = 4017 - 1.255T, \tag{9}$$

$$L_{\mathrm{Cu,Fe}} = 41033.0 - 6.022T, \tag{10}$$

$$T_{\mathrm{c}} = 1043(1 - C_{\mathrm{Cu}}) - 580C_{\mathrm{Cu}}, \tag{11}$$

$$\beta^\alpha = 2.22(1 - C_{\mathrm{Cu}}). \tag{12}$$

The function of $f(\tau)$ is given by Hillert and Jarl [31] as:

$$f(\tau) = 1 - \frac{1}{D}\left\{\frac{79\tau^{-1}}{140p} + \frac{474}{497}\left(\frac{1}{p} - 1\right)\left(\frac{\tau^3}{6} + \frac{\tau^9}{135} + \frac{\tau^{15}}{600}\right)\right\}, \quad (\tau \leqslant 1),$$

$$f(\tau) = -\frac{1}{B}\left(\frac{\tau^{-5}}{10} + \frac{\tau^{-15}}{315} + \frac{\tau^{-25}}{1500}\right), \quad (\tau > 1),$$

$$B = \frac{518}{1125} + \frac{11692}{15975}\left(\frac{1}{p} - 1\right), \quad (p = 0.4 \text{ for the bcc phase}). \tag{13}$$

For a given temperature, the chemical free energy can be plotted, as shown in figure 1. For a given temperature and Cu concentration, we can obtain the equilibrium concentration and the spinodal decomposition concentration of this Fe–Cu system, as shown in table 1. In table 1, the equilibrium Cu concentration means the concentration of Cu clusters will grow to

Table 1. Equilibrium and spinodal decomposition concentrations for Fe–Cu binary alloy.

Temperature (K)	Equilibrium concentration		Spinodal decomposition
	Solution	Cu precipitate	Concentration
550	0.6×10^{-3}	0.999	0.06 0.94
650	1.5×10^{-3}	0.998	0.07 0.93
773	3.6×10^{-3}	0.996	0.10 0.90
950	0.01	0.990	0.13 0.87
1150	0.03	0.970	0.16 0.84

Table 2. Diffusion coefficients of different elements.

Element	D ($T = 550$ K)	D ($T = 650$ K)
Fe	7.2×10^{-32}	4.2×10^{-27}
Cu	5.0×10^{-29}	8.0×10^{-25}

that equilibrium state, and the spinodal decomposition is a mechanism for the rapid un-mixing of a Fe–Cu mixture system, with Cu concentration higher than that of spinodal decomposition concentration. Cu-rich clusters will form by nucleation and growth processes when the concentration of Cu if less than the spinodal decomposition concentration.

2.3. Interfacial energy coefficient and diffusion coefficient

In the phase field model described in equations (1)–(4), both the chemical free energy $G(C_{Cu}, T)$ and the gradient energy contribute to the interfacial energy. So a numerical method is used to determine the concentration gradient energy coefficients for a given interfacial energy γ and interfacial thickness λ. The numerical value of the composition gradient energy coefficient can be estimates as $\kappa_{Cu} = 1/2\Omega d^2$ [32], where Ω is an interaction parameter between atoms and we use $\Omega = L_{Cu,Fe}(T = 0 \text{ K}) = 41\,033.0$ (J mol^{-1}) (see equation (10)). d is an effective interaction distance [33], which is assumed as $d = 0.7$ (nm). This value is about a half length of the interface region between the Cu-precipitate and the matrix. Then we have $\kappa_{Cu} = 1.0 \times 10^{-14}$ (J m^2 mol^{-1}) for $\gamma = 1$ J m^{-2} and $\lambda = 3l_0$.

On the other hand, the diffusion coefficient in solids at different temperatures is needed to solve the equations (1)–(4), as well. These parameters are generally found to be well predicted by the Arrhenius equation:

$$D = D_0 e^{E_A/kT},$$

where D is the diffusion coefficient, D_0 is the maximum diffusion coefficient, T is the temperature, k is the Boltzmann constant, and E_A is the diffusion activation energy. For bcc Fe alloys, these parameters of different elements diffusion coefficient by a vacancy mechanism can be adapted from the [34] and listed in table 2 ($T = 550, 650$ K).

Modelling Simul. Mater. Sci. Eng. **25** (2017) 085006

B Li *et al*

2.4. String method

To compute the MEP and the critical nucleus, we apply the constrained string method developed by Du and Zhang [35]. The string method was first proposed by Ren and Vanden-Eijnden in [15, 16], and it has been successfully used for nucleation in solids [17, 18] and phase transformations [19].

The string method proceeds by evolving a string, i.e., a smooth curve with intrinsic parametrization, to the MEP between two metastable/stable states in the configuration space. Specifically, let $\phi(\alpha, t)$ denote the string at the time t with parametrization $\alpha \in [0, 1]$, then the simplified string method [16] is to evolve the string according to

$$\varphi_t(\alpha, t) = -\nabla E(\varphi) + \lambda \hat{\tau},$$

where $\hat{\tau}$ is the unit tangent vector to the string, i.e., $\hat{\tau} = \varphi_\alpha / |\varphi_\alpha|$. λ is the Lagrange multiplier to impose the equal arc-length constraint. The above equation is supplemented with the boundary conditions:

$$\phi(0, t) = C_{eq}^0, \quad \varphi(0, t) = C_{eq}^1,$$

where C_{eq}^0 and C_{eq}^1 are two equilibriums of the energy.

For a conserved concentration field, the computation of MEP and critical nucleus is subject to the constraint $\int_\Omega (C(x) - C_0) \mathrm{d}x = 0$, with C_0 is the concentration for the homogeneous state. The constrained string method can be applied to solve the constrained MEP [35]. Then the critical nucleus is the image with the highest energy along the MEP since it is the maximum along the path direction and the minimum along the other directions.

The constrained string method allows several equivalent formulations such as the Lagrange multiplier method or the augmented Lagrange multiplier method. Yet, some formulations are more natural and robust than others and require less parameter turning. In particular, one effective approach is to apply Cahn–Hilliard type dynamics rather than the Allen–Cahn dynamics with additional Lagrange multiplier. The Allen–Cahn equation refers to the standard L^2 inner product while the Cahn–Hilliard equation uses the H^{-1} inner product. Hence, we now introduce the constrained string method as follows:

$$\varphi_t(\alpha, t) = -\nabla^2 \frac{\delta E(\varphi)}{\delta \varphi} + \lambda \hat{\tau}.$$

In the numerical implementation, the discretized string is composed of a number of images $\{\varphi(i, t), i = 0, 1, \ldots, N\}$. Then we can use a time splitting scheme via the following iterations:

Step 1 (string evolution): We update the images on the string over some time interval Δt according to

$$\phi_t(i) = -\nabla^2 \frac{\delta E(\varphi(i))}{\delta \varphi}, \quad i = 1, 2, \ldots, N - 1.$$

Step 2 (string re-parametrization): After the string is updated by Step 1, we apply linear or cubic interpolation by equal arc length to redistribute the images along the string to obtain the new discretized string with equal distance.
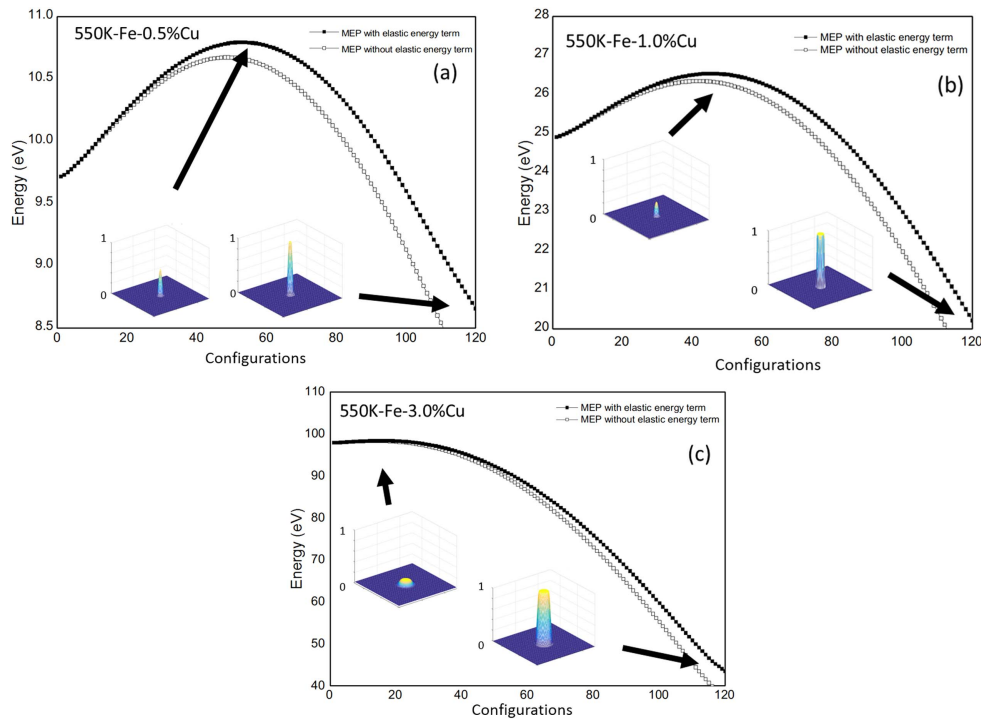
Figure 2. Critical nucleus, equilibrium and MEP for Fe–Cu alloys at 550 K. (a) 550 K, Fe-0.5%Cu (b) 550 K, Fe-1.0%Cu (c) 550 K, Fe-3.0%Cu (solid line for considering elastic energy and open line for not).

3. Results and discussion

The nucleus of Cu clusters in Fe will be a sphere in a real three dimensional space, and experiments have proved that [36, 37]. In this work, we consider a 2D simulation cell of $128l_0 \times 128l_0$ ($l_0 = 0.2$ nm in this work) for simplification.

The critical nucleus will change with the temperature and Cu overall concentration because of the chemical free energy in equation (4) depending on the Cu overall concentration and temperature. Here we consider two different temperatures 550 K/773 K, and three Cu overall concentration of 0.5%, 1.0% and 3.0%. For a given temperature (T) and Cu overall concentration C_{Cu0}, we can obtain the critical nucleus, the final Cu cluster and the energy path for this progress.

We can see that the concentrations inside the nuclei are much smaller than the equilibrium concentration of Cu precipitates ($C_{Cu} \approx 1$) that are calculated from the equilibrium phase diagram. Experiments of atom probe observation [36, 37] have also demonstrated that the Cu concentration in the nuclei does not have to be its bulk equilibrium value; therefore, the critical nucleus of Cu precipitate is non-classical. Although it is hard to define the critical size of a nucleus, we can clearly see that Cu concentration inside the critical nuclei increases with the decrease of the Cu overall concentration or the increase of temperature. That is to say, it is more stable for Cu to precipitate in Fe–Cu system in a lower temperature or higher Cu overall concentration.

The concentration of Cu nucleus and the energy for nucleation are calculated from the Cahn–Hilliard non-classical nucleation theory. In figures 2(a)–(c), for $T = 550$ K and
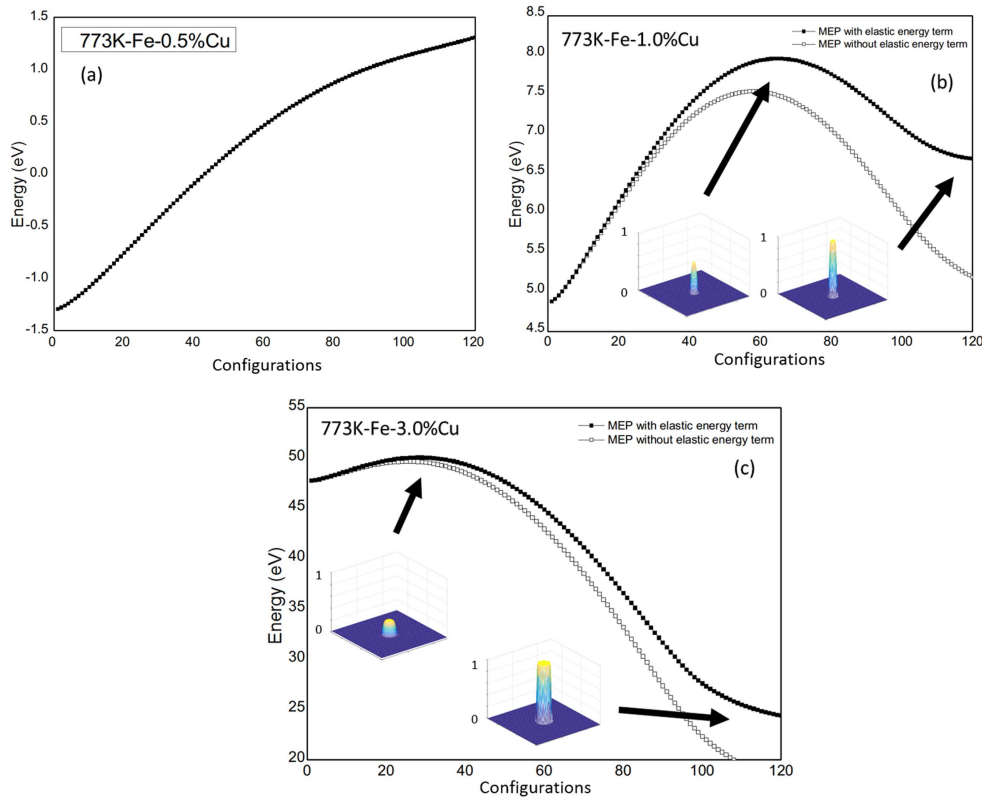
Figure 3. Critical nucleus, equilibrium and MEP for Fe–Cu alloys at 773 K. (a) 773 K, Fe-0.5%Cu (b) 773 K, Fe-1.0%Cu (c) 773 K, Fe-3.0%Cu (solid line for considering elastic energy and open line for not).

Table 3. Thermodynamic properties of critical nucleus.

Temperature (K)	Cu concentration (at%)	Initial energy (eV)	Energy barrier (eV)	Final energy (eV)	Cu concentration in critical nucleation (at%)
550	0.5	9.72	1.08	8.66	56
	1.0	24.92	1.62	20.22	37
	3.0	97.94	0.49	43.54	17
773	0.5	−1.29	*	*	*
	1.0	4.89	3.08	6.69	69
	3.0	47.76	2.30	24.43	34

$C_{Cu0} = 0.5,\ 1.0,\ 3.0$, we plot the MEP and insert both the critical nucleus and the equilibrium precipitate on the string. The X axis represents the configuration along the MEP. In particular, 0 represents the initial homogeneous configuration, 120 stands for the equilibrium precipitate, and the configuration with the highest energy corresponds to the critical nucleus. Another example is figures 3(a)–(c), for $T = 773$ K and $C_{Cu0} = 0.5,\ 1.0,\ 3.0$. One of the interesting observations is for $T = 773$ K and $C_{Cu0} = 0.5\%$, the Cu clusters would not be

stable, the energy per atom is increasing for any Cu segregation (so here we did not draw the MEP without consideration of elastic energy). Therefore, with a lower Cu average concentration and a higher temperature, there are possibilities that Cu would not segregate. With section 2.4, it is known that the critical nucleus is associated with the concentration fluctuation that has the minimum free energy increase amongst all of the fluctuations that lead to growth. We list the thermodynamic properties of critical nucleus in table 3, including the energy barrier and Cu concentrations in critical nucleation for different temperatures and Cu overall concentrations. It is easy to find that both the nucleation barrier and the maximum value of a critical nucleus strongly depend on the temperature and Cu concentration. It is clearly seen that the nucleation barrier decreases with decreasing temperature and increasing average Cu concentration. This is in agreement with the spinodal decomposition theory. These thermodynamic properties are important to calculate the nucleation rates and introduce the correct critical nuclei in the phase-field modeling of precipitation kinetics.

4. Conclusions

With the thermodynamic and kinetic properties of Fe–Cu binary alloys from CALPHAD, the phase-field model coupled with the constrained string method have been successfully applied to quantitatively predict the concentration profiles of critical nuclei, nucleation energy barriers, and equilibrium of Cu precipitates in Fe–Cu binary alloys. The phase field approach is used to describe the effect of radiation damage or aging on phase stability and microstructure evolution while the constrained string method is applied to obtain the MEP. These results are in agreement with experiment results (both aging and radiation damage sample) and simulation results.

The simulations of critical nuclei showed a number of interesting phenomena, including:

(1) The formation of Cu stable clusters needs to overcome an energy barrier calculated with Cahn–Hilliard non-classical nucleation theory.
(2) The concentration of the critical nucleus of Cu decreases with the decrease of the temperature or the increase of overall Cu concentration in the matrix.
(3) The relative energy barrier for forming a stable Cu cluster increases with the increase of the temperature or the decrease of overall Cu concentration in the matrix.

All these results are in agreement with experimental results (both aging and radiation damage sample) and simulation results [2, 13, 14, 27, 38]. The obtained thermodynamic properties are important to calculate the nucleation rates and introduce the accurate critical nuclei in the phase-field modeling of precipitation kinetics, which is essential to study the evolution kinetics of precipitates.

Acknowledgments

ORCID iDs

Boyan Li ⓘ https://orcid.org/0000-0002-9665-3799

References

[1] Goodman S R, Brenner S S and Low J R Jr 1973 *Metall. Trans.* **4** 2363–9
[2] Deschamps A, Militzer M and Poole W J 2001 Precipitation kinetics and strengthening of a Fe-0.8wt%Cu Alloy *ISIJ Int.* **41** 196–205
[3] Eason E D, Odette G R, Nanstad R K *et al* 2013 A physically-based correlation of irradiation-induced transition temperature shifts for RPV steels *J. Nucl. Mater.* **433** 240–54
[4] Odette G R and Lucas G E 1998 Recent progress in understanding reactor pressure vessel steel embrittlement *Radiat. Eff. Defects Solids* **144** 189–231
[5] Fisher S B, Harbottle J E and Aldridge N 1985 Radiation hardening in magnox pressure-vessel steels *Phil. Trans. R. Soc.* A **315** 301–32
[6] Nagai Y *et al* 2001 Irradiation-induced Cu aggregations in Fe: an origin of embrittlement of reactor pressure vessel steels *Phys. Rev.* B **63** 134110
[7] Pareige P 1996 Characterization of neutron-induced copper-enriched clusters in pressure vessel steel weld: an APFIM study *Appl. Surf. Sci.* **94–95** 370–7
[8] Tobita T *et al* 2014 Effects of irradiation induced Cu clustering on Vickers hardness and electrical resistivity of Fe–Cu model alloys *J. Nucl. Mater.* **452** 241–7
[9] Li Y L, Hu S Y, Sun X and Stan M 2017 A review: applications of the phase field method in predicting microstructure and property evolution of irradiated nuclear materials *npj Comput. Mater.* **3** 16
[10] Chen L Q 2002 Phase-field models for microstructure evolution *Annu. Rev. Mater. Res.* **32** 113–40
[11] Steinbach I 2009 Phase-field models in materials science *Modelling Simul. Mater. Sci. Eng.* **17** 073001
[12] Hu S and Henager C H 2009 Phase-field modeling of void lattice formation under irradiation *J. Nucl. Mater.* **394** 155–9
[13] Zhang C and Enomoto M 2006 Study of the influence of alloying elements on Cu precipitation in steel by non-classical nucleation theory *Acta Mater.* **54** 4183–91
[14] Zhang C *et al* 2004 Cu precipitation in a prestrained Fe-1.5 wt pct Cu alloy during isothermal aging *Metall. Mater. Trans.* A **35** 1263–72
[15] Weinan E, Weiqing R and Vanden-Eijnden E 2002 String method for the study of rare events *Phys. Rev.* B **66** 052301
[16] Weinan E, Weiqing R and Vanden-Eijnden E 2007 Simplified and improved string method for computing the minimum energy paths in barrier-crossing events *J. Chem. Phys.* **126** 164103
[17] Zhang L, Chen L-Q and Du Q 2010 Simultaneous prediction of morphologies of a critical nucleus and an equilibrium precipitate in solids *Commun. Comput. Phys.* **7** 674–82
[18] Zhang L, Chen L-Q and Du Q 2010 Diffuse-interface approach to predicting morphologies of critical nucleus and equilibrium structure for cubic to tetragonal transformations *J. Comput. Phys.* **229** 6574–84
[19] Zhang L, Ren W, Samanta A and Du Q 2016 Recent developments in computational modeling of nucleation in phase transformations *npj Comput. Mater.* **2** 16003
[20] Zhang L, Chen L Q and Du Q 2007 Morphology of critical nuclei in solid-state phase transformations *Phys. Rev. Lett.* **98** 1–4
[21] Shen C, Li J and Wang Y Z 2008 Finding critical nucleus in solid-state transformations *Metall. Mater. Trans.* A **39A** 976–83
[22] Philippe T and Blavette D 2011 Nucleation pathway in coherent precipitation *Phil. Mag.* **91** 4606–22
[23] Heo T W and Chen L Q 2014 Phase-field modeling of nucleation in solid-state phase transformations *JOM* **66** 1520–8
[24] Poduri R and Chen L Q 1996 Non-classical nucleation theory of ordered intermetallic precipitates-application to the Al–Li alloy *Acta Mater.* **44** 4253–9
[25] L'Vov P E and Svetukhin V V 2015 Simulation of nonclassical nucleation in binary alloys *Phys. Solid State* **57** 1213–22

[26] Koyama T, Hashimoto K and Onodera H 2006 Phase-field simulation of phase transformation in Fe–Cu–Mn–Ni quaternary alloy *Mater. Trans.* **47** 2765–72

[27] Koyama T and Onodera H 2005 Computer simulation of phase decomposition in Fe–Cu–Mn–Ni quaternary alloy based on the phase-field method *Mater. Trans.* **46** 1187–92

[28] Saunders N and Miodownik A P (ed) 1998 *CALPHAD (Calculation of Phase Diagrams): A Comprehensive Guide* vol 1 (Amsterdam: Elsevier) pp 153–62

[29] Dinsdale A T 1991 SGTE data for pure elements *CALPHAD* **15** 317–425

[30] Miettinen J 2003 Thermodynamic description of the Cu–Fe–Mn system at the Cu–Fe side *CALPHAD* **27** 141–5

[31] Hillert M and Jarl M 1978 A model for alloying in ferromagnetic metals *CALPHAD* **2** 227–38

[32] Cahn J W 1998 *The Selected Works of J. W. Cahn* ed W C Carter and W C Johnaon (Pennsylvania: TMS) p 29

[33] Miller M K, Wirth B D and Odette G R 2003 *Mater. Sci. Eng.* A **353** 133

[34] Messina L, Nastar M, Sandberg N *et al* 2016 Systematic electronic-structure investigation of substitutional impurity diffusion and flux coupling in bcc iron *Phys. Rev.* B **93** 184302

[35] Du Q and Zhang L 2009 A constrained string method and its numerical analysis *Commun. Math. Sci.* **7** 1039–51

[36] Miller M K and Russell K F 2007 Embrittlement of RPV steels: an atom probe tomography perspective *J. Nucl. Mater.* **371** 145–60

[37] Miller M K, Wirth B D and Odette G R 2003 Precipitation in neutron-irradiated Fe–Cu and Fe–Cu–Mn model alloys: a comparison of APT and SANS data *Mater. Sci. Eng.* A **353** 133–9

[38] Li Y, Hu S, Zhang L and Sun X 2014 Non-classical nuclei and growth kinetics of Cr precipitates in FeCr alloys during ageing *Modelling Simul. Mater. Sci. Eng.* **22** 25002